18

Regional Pattern of Trends in Long-Term Precipitation and Stream Flow Observations: Singularities in a Changing Climate in Mexico

Luis Brito Castillo
Centro de Investigaciones Biológicas del Noroeste
Mexico

1. Introduction

The Intergovernmental Panel on Climate change has concluded that global warming is unequivocal (IPCC, 2007). However, there is still a debate regarding whether global warming is mainly due to anthropogenic greenhouse gas emissions (Zhao, 2011), particularly because, as Lindzen (2007) states, current models fail to describe many known climate changes, and because some sources of anthropogenic forcing contribution (like surface albedo, total aerosol, etc) are essentially unknown (Lindzen, 2007). It has been stated that the warming has penetrated into the world's oceans (Barnett et al., 2005) increasing sea surface temperatures (SSTs) by approximately 0.5°C since the mid-nineteenth century (Houghton et al. 2001). Higher SSTs are associated with increased water vapor in the lower troposphere (Trenberth, 2005) implying that perturbations in the global water cycle are expected to accompany this warming (Milly et al., 2005). The understanding of specific regional changes (i.e. trend analysis) in temperature, rainfall, and streamflow is very necessary for supporting the needs of an ever-broadening spectrum of decision-makers as they strive to deal with influences of Earth's climate at global to local scales. Trend analyses have revealed the existence of temperature trends with different signs in Mexico in general (Englehart & Douglas, 2004; Pavia et al., 2009), central Mexico (Brito-Castillo *et al*., 2009), and northwestern Mexico (Gutierrez-Ruacho et al., 2010; Weiss & Overpeck, 2005), which is partly associated with regional land use, changes in land cover (Englehart & Douglas, 2004), and changes in large-scale atmospheric flow patterns (Brito-Castillo *et al*., 2009). These studies have shown that, while significant trends do exist, they are at times in line with warming hypotheses and at times they are not. The complete understanding of these changes is particularly important, especially for river discharges, since availability of water is vital for human health, economic activity, ecosystem functions, and geophysical processes (Milly et al., 2005). In Mexico, trend analyses have mostly focused on maximum and minimum temperatures, while trend analyses of precipitation and streamflow have only partly been studied. Knowledge remains scarce, partly attributed to lack of long-term data (both in space and time), the difficulties encountered in providing a correct interpretation of changes attributed to human disturbances, such as diversion of water for irrigation of cropland and control of water for generating electric power, as well as the complexity of the processes that externally force hydroclimate variability (natural changes and low-frequency

internal variability, such as Pacific decadal oscillation (PDO) and Atlantic multidecadal oscillation (AMO). Given the limited knowledge of streamflow and precipitation trend structures in Mexico, in this chapter, we analyzed overall trends in Mexico and described the regional structures of the trends for the period 1920–2008. Evidence of real trends over different regions of Mexico is provided, sometimes revealing that oscillations of long-term high and low humid periods (depending on their arrangement) force the fitted linear trend model. This implies that declining or increasing trends are restrained by the length of the records. However, there are also cases of unambiguous multi-decadal trends in rainfall and streamflow time series that require more detailed analysis. Section 2 explains the statistical approaches used in the study of trends, with some real examples from precipitation and streamflow variables in Mexico. In Section 3, we describe seasonal precipitation characteristics over Mexico to illustrate the main climate differences across the country. Section 4 provides an introduction to the most recent findings related to global warming and changes in tropical cyclones, including a brief description of tropical cyclone contribution to rainfall in Mexico. In the remaining sections, we explain the main procedures for detecting trends used in this work. In Section 5 we describe climate data and quality control; in Section 6, we show a regionalization of Mexico by simply fractioning the territory into several domains with specific climatic conditions. Finally, in Sections 7 and 8, we discuss the main regional structures of trends detected in precipitation variables and their correspondence to trends in streamflow datasets. We hope that this chapter provides a useful introduction to problems related to trends in precipitation and streamflow variables in Mexico.

2. The study of trends

If data show continuous increase or decline change over time, we refer to this change as a trend (Figure 1). Linear trends are an example of data "statistics" like the average (or mean) and "standard deviation values", which is a measure of the variability within a data set around the mean value. Sometimes, to allow comparisons between the series having different scales of variability results, it is necessary to change the data scores to standardized values or z scores, which is the number of standard deviations away from the mean:

$$z_i = (x_i - \mu) / \sigma \quad (1)$$

where: z_i, is the standard score; x_i is the observed score; μ is the mean value; σ is the standard deviation; i = 1…n; and n is the sample size.

When all the scores from a variable are transformed into standard scores (z scores), a new variable is obtained with a mean of zero and standard deviation of one.

Fitting a linear trend model to data is a common practice; however linear trends may be deceptive, particularly when datasets show non-linear changes over time (Wigley, 2006), which is a property of precipitation and streamflow time series. An example of this situation is displayed in Figure 1 for three different series expressed as z scores: (1) Total annual days with precipitation >0 mm (i.e. annual TDP > 0) (Figure 1a); (2) Total annual precipitation (mm) (Figure 1b & Figure 2) and (3) mean annual streamflow (m^3/s) (Figure 1c). All variables show an initial declining trend (though incomplete), followed by a large upward step after 1958 that results in an overall increasing trend. It is evident that inter-annual variability of the time

series is superimposed on multi-decadal variability with substantial deviations from linearity (i.e., the trend) in some years (1956 and 2000 in Figure 1b and in 1959 and 2004 in Figure 1c.). In these situations a detailed inspection of the series can help show more complex changes that are evident in data; still, linear trends provide the simplest and most convenient way to describe the overall change over time in a dataset (Wigley, 2006).

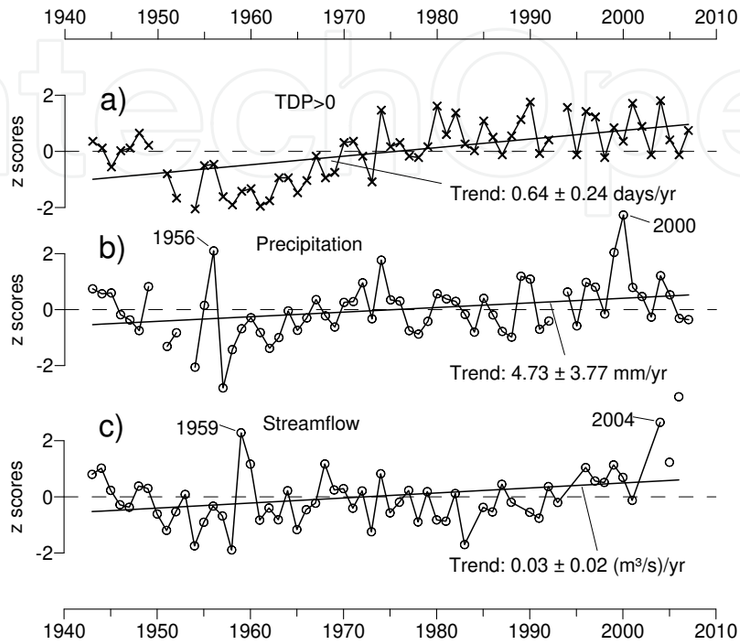

Fig. 1. Long-term fluctuations of different data sets: (a) Total annual days with precipitation >0 mm (TDP >0); (b) total annual precipitation (mm) and (c) mean annual streamflow (m^3/s). a-b are from Ocozonautla, Chiapas weather station (Code: 07123; –93.374°W; 16.751°N; 838 masl); c is from La Y-Rio Lerma gauging station (Code: 12374; –99.5894°W; 19.40611°N; basin area 1582 km^2). The line is the trend and the ± values define the 95% confidence intervals for the trends. For comparison all variables are expressed in standardized values (i.e., z scores; see text for definitions).

In this work, linear trends were quantified as the change of TDP > 0, precipitation, and streamflow per year by fitting a straight line to the data using the method of minimal least squares errors, with years (T) as the independent values and serial data (Y) within each year as the dependent values. The "best-fit" straight line to data is obtained by linear regression analysis:

$$Y_{est} = b + T \tag{2}$$

$$b = [\sum\{(T_i - T_{avg})\,(Y_i - Y_{avg})\}] \,/\, [\sum\{(T_i - T_{avg})^2\}], \tag{3}$$

where $\sum$ represents the summation over i = 1…n; the subscripts "est" and "avg" are the estimate of Y (TDP > 0, precipitation or streamflow) by the fitted regression line and the mean value, respectively, and b is the slope of the fitted line (the trend value).

Estimates of the linear trend are sensitive to points at the start or end of the dataset. This is more a problem with small sample sizes (for trends over short time periods). For example, if

we considered streamflow data points in Figure 1c from 1959 through 1983 (25 years), because there was an unusual increase in 1959 (which is also recorded at other gauging stations downstream along the river), the calculated trend may be an overestimate of the true underlying trend.

Other uncertainties that can be found in trend analysis is related to the presence of gaps in datasets and the apparently multi-decadal variability that seems to be "incomplete" in some series (Figure 2), giving the impression that the trends might not be real. In both cases shown in Figure 2, there are clear trends, upward trend in Figure 2a and downward trend in Figure 2b. However, after the 1970s, the overall trend in Figure 2a assumes a decreasing trend. Unfortunately, the dataset finished very early at the middle of the 1990s without enough data to prove if this second trend is statistically significant (see below for definition). In Figure 2b, on the contrary, there is an overall decreasing trend, but before 1970, it seems to be an increasing trend or no trend at all. Unfortunately, the dataset beginning in 1950 cannot prove this. Around the 1970s, the scores are greater than the mean value in both datasets (Figures 2a & b). Comparing the overall behavior between both data sets, it seems as though both datasets were complementary to each other, indicating the possibility that, if observations were available for both time series over the 1920-2010 period, it might be possible to calculate no trend at all. So far, we can say that, with this information, increasing (Figure 2a) or declining (Figure 2b) trends might be restrained by the length of the records.

For examples, given in Figure 2, results necessary to explore the behavior of surrounded stations is more certain.

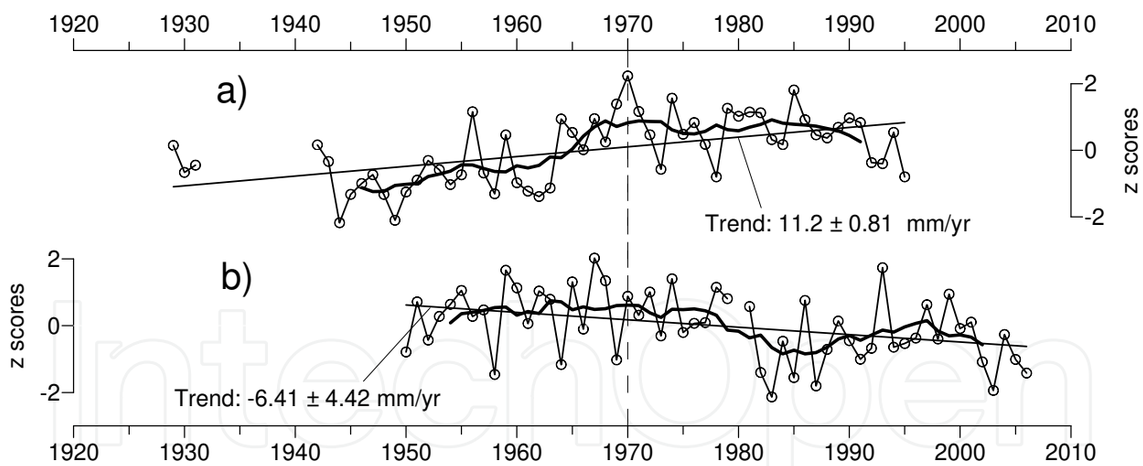

Fig. 2. The same as Figure 1, but for total annual precipitation (mm). (a) Matías Romero (Code: 20068; –95.03°W; 16.88°N; 201 masl); (b) Paso de Arocha, Nayarit Code: 18025; –105.10°W; 21.83°N; 30 masl). Heavy lines are 9-yr running means.

A measure of how well the straight line fits the data is the average value of the squares of the residuals (i.e. deviations about the fitted line) or the standard deviation of the trend estimate, or its squares, the variance of the distribution of b (Var(b)). The smaller this is, the better is the fit:

$$\mathrm{Var}(b) = (\mathrm{SE})^2 = \mathrm{MSE} \,/\, [\sum\{(T - T_{avg})^2\}] \quad (4)$$

$$MSE = [\sum((Y - Y_{est})^2)] / (n - 2) \quad (5)$$

where MSE is the mean square error and SE is the standard error of the trend estimate.

To decide if upward or downward trends are an indication of some underlying cause or merely a chance fluctuation, in this work, we use two approaches: (1) confidence intervals: b ± 2 SE (often called the two-sigma confidence interval) and (2) significance testing. The range b ± 2 SE is a good approximation to represent the 95% confidence interval and is used as a signed error magnitude. If –2SE < b < 2SE, it means that the 95% confidence interval includes the zero trend value and the null hypothesis that "there is no trend in data sets or b = 0" is true; otherwise (i.e. b > 2SE or b < –2SE), we say that the null hypothesis is unlikely to be true and we must accept the alternate hypothesis that "data show a real, externally forced upward or downward trend (Wigley, 2006).

The second approach consists in trying to decide whether an observed data trend that is noticeably different from zero is sufficiently different that it could not have occurred by chance or that the probability (known as p-level) that it could have occurred by chance is very small. If the null hypothesis is rejected, then we say that the observed trend is "statistically significant" at some level of confidence. In this study, the confidence level we used to reject the null hypothesis is alpha level = 0.05. If the probability that the null hypothesis is true is small (i.e. p-level < 0.05), then the null hypothesis is unlikely to be correct. Such a low probability would mean that the observed trend is highly unusual and therefore a "significant result". The significance test used here is a "two-tailed" test, meaning that we are concerned only with whether the trend is different from zero, with no specification of whether the trend should be increasing (positive) or declining (negative) trend.

The significance of a trend and its confidence intervals depend on the standard error of the trend estimate. Equation (4) given above is, however, only correct if the individual scores are unrelated. The dependence between scores is referred to as "temporal autocorrelation" or "serial correlation". When data are auto-correlated, many statistics behave as if the sample size was less than the number of data points, n, so it is necessary to determine an "effective sample size" (n_{eff}). In this study, n_{eff} was estimated by Equation (6):

$$n_{eff} = n(1 - r_1) / (1 + r_1) \quad (6)$$

where r_1 is the lag-1 autocorrelation coefficient calculated from the time series of residuals about the fitted line of the observed data.

If r_1 is statistically significant (i.e. p-level of r_1 is < 0.05), then in Equation (5), n_{eff} is used instead of n. It can be seen from Equation (5) that if n_{eff} is noticeably smaller than n, then the standard error of the trend estimate may be much larger than one would otherwise expect. This means that results that may show a significant trend if autocorrelation is ignored; it is frequently found to be non-significant when autocorrelation is accounted for.

3. Rainfall distribution over Mexico

The climate of Mexico is influenced by the strength and position of the subtropical high pressure systems of the Northeast Pacific (the East Pacific High) and the North Atlantic (the Bermuda High) (Wang et al., 2007), and the variations in the location of the Intertropical Convergence Zone (ITCZ), which lies south of Mexico. The formation of the high pressure

systems is related to global scale circulations that function to move excess energy from the equatorial regions to poles affecting precipitation variability across Mexico on seasonal to decadal time scales. An unusually strong East Pacific High during the winter can steer storm systems far to the north, limiting cloud formation and precipitation with a drying effect over the river basins in much of northern Mexico (Brito-Castillo et al., 2003), while an unusually strong Bermuda High during the summer can enhance monsoon circulation and numerous transient disturbances (e.g. tropical storms, tropical easterly waves, inverted troughs, the Madden Julian Oscillation, and mid-latitude troughs) and bring above-average precipitation across much of Mexico (Douglas et al., 2007; Wang et al., 2007). Subtle changes to the position and strength of these circulation features appear to be connected to global scale shifts in circulation patterns related to changes in sea surface temperature patterns (e.g., El Niño-Southern Oscillation) affecting rainfall variability of Mexico at inter-annual timescales and can persist for years (e.g., the Pacific Decadal Oscillation, PDO), bringing extended periods of unusually wet or dry conditions at decadal timescales (Magaña et al., 2003; Pavia et al., 2006).

3.1 Seasonality of precipitation

Mexico receives most of its annual rainfall during the summer, with a secondary peak occurring during the winter. From November through March (Figure 3 left maps), winter precipitation is associated with large-scale low pressure systems that traverse northern Mexico, drawing in moisture from the Pacific Ocean and producing widespread rain and snow at higher elevations of the Sierra Madre Occidental in northwestern Mexico, the northwestern portion of the Baja California Peninsula, the coastal plains of the Gulf of Mexico (CPGM), the Yucatan Peninsula (YP), and some portions of central Mexico (mainly in December and January), while the rest of the country generally experiences dry conditions. The effects of cold fronts coming from the northwest also cause lower temperatures in most of Mexico, but are more evident in the highlands of north and central Mexico, and on the CPGM, and the YP, where they are associated with strong northerly winds (nortes; outbreaks of cold weather), occasionally producing intense precipitation in the southeast, when the cold air masses are modified by the warm waters from the Gulf of Mexico. The large-scale forcing (1000 km-global) of regional climate variability, such as the location and strength of the subtropical westerly jet, determines the succession of weather events during winter in eastern Mexico. A change from zonal to more frequent meridional circulation has been linked to increased winter precipitation over the region. At the end of March, the strong midlatitude westerlies (jet stream) begin their northward retreat, and more tropical conditions affect the region, restraining wet conditions mostly over the CPGM and YP during April (Figure 3 left maps).

Summer precipitation in Mexico (May through October, see Figure 3 right maps) is, in large part, controlled by the North American Monsoon (NAM) system (Higgins et al., 2003), which is associated with thermal contrasts between the continent and adjacent eastern Pacific Ocean (Giovannettone & Barros, 2008; Higgins et al., 2003; Turrent & Cavazos, 2009).

Initially, greater rainfall occurs in southern Mexico in May, as the ITCZ assumes a northerly position during the Northern Hemisphere summer. This position, combined with modulation by easterly waves from the Caribbean Sea and the lower branch of easterly flow from over the Gulf of Mexico have a direct influence on the mountain ranges in southern Mexico (Giovannettone & Barros, 2007), initiating precipitation over the southern slopes and

propagating northward as the convective activity and easterlies strengthened in May-June. In southern and central Mexico, precipitation peaks in June and September with a decline in convective activity in late July-early August, causing a break period known as canicula (midsummer drought) (Magaña et al., 1999), as a result of the presence of an anticyclone southwest of Mexico over the ITCZ (Giovannettone & Barros, 2007).

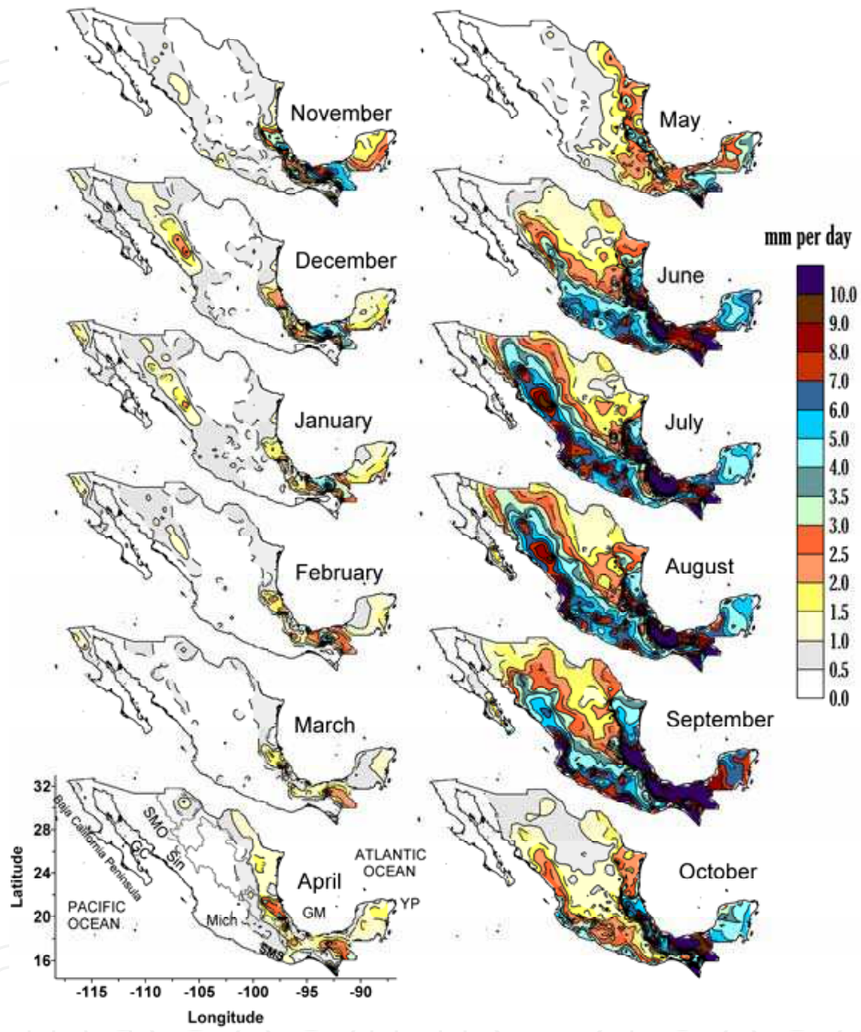

Fig. 3. Distribution of long-term mean values of daily precipitation per month. The mean value is calculated for individual stations with larger than 40 yrs of records over the 1948–2000 period. In lower left map, GC = Gulf of California; Sin = Sinaloa; Mich = Michoacan; SMO = Sierra Madre Occidental; SMS = Sierra Madre del Sur, GM = Gulf of Mexico, YP = Yucatan Peninsula.

Poleward extension of the summer precipitation regime in northwest Mexico starts with an abrupt onset of precipitation in late June or early July and quickly spreads northward along the western slopes of the Sierra Madre Occidental. Precipitation increases coincide with increased vertical transport of moisture by convection and southerly winds through the Gulf of California. During July through early September, the monsoon system is fully developed

and the heaviest rainfalls occur west of the Sierra Madre Occidental. In late September to October, precipitation over northwest Mexico diminishes in response to a southward movement of the NAM upper level anticyclone to weakening of land surface heating and southerly flow and to the retraction of the North Atlantic Subtropical High eastward.

Other sources of moisture in Mexico during summertime are mesoscale convective systems (Farfan & Zhender, 1994) and tropical cyclones (Farfan, 2011; Jáuregui, 2003).

4. Tropical cyclones and their contribution to rainfall

It has been established that sea surface temperature (SST) is increasing all over the world (Barnett et al., 2005). For tropical SSTs, the total increase has been on the order of 0.5°C since the mid-nineteenth century (Houghton et al. 2001). Warming signals have been found to be far stronger than would be expected from natural internal variability (i.e., external forcing such as solar variability or volcanic activity), attributing ocean warming signal to anthropogenic forcing (Barnett et al., 2005). A warmer tropical ocean brings increased water vapor in the lower troposphere and both tend to enhance moisture convergence for a given amount of mass convergence. This increases the energy available for atmospheric convection and rainfall rates in systems, such as thunderstorm and cyclones (Knutson et al., 2010) where moisture convergence is an important component of the water-vapor budget. However, the issue of attribution of increased hurricane frequency to increasing SST has been a matter of academic debate, since there is no sound theoretical basis for drawing any conclusions about how anthropogenic climate change affects hurricane number or tracks (Trenberth, 2005). It is known than over the 20th century, there is a nonlinear upward trend in SSTs with domination of multi-decadal variability being a pronounced trend in the past three to four decades (Trenberth, 2005). The study by Webster et al. (2005), analyzing global hurricane data, shows that, opposed to increasing SST, no global trend has yet emerged in the number of tropical storms or hurricanes, although model results and observations suggest a shift in hurricane intensities toward extreme hurricanes (Knutson et al., 2010; Webster et al., 2005; Yu et al., 2010).

With extensive coastline bordering both oceans, Mexico is particularly vulnerable to hurricanes. Moreover, the eastern Pacific Ocean is the most productive in hurricane activity of any basin per unit area worldwide (McBride, 1995). From May through October, an average of 15 named tropical cyclones (TC) form every summer season and provide changes in moisture content to western Mexico (Farfan, 2011). According to Jáuregui (2003), from 1951–2000, Pacific hurricane hits were more frequent on coastal areas of Sinaloa, southern Baja California Peninsula, and Michoacan. More recently, analysis by Farfan (2011) states that, from 1970 through 2009, the Baja California Peninsula was the most affected area, with 97% probability of being affected by at least one TC each season and 46% probability of having at least one TC move inland. On the Atlantic side, the Yucatan Peninsula and the northern state of Tamaulipas were the most exposed to these storms (Jáuregui, 2003). September is the month with the highest rate (33% compared to the eastern Pacific Ocean) of landfall in Mexico (Diaz et al., 2008; Farfan, 2011; Jáuregui, 2003). The study made by Jáuregui (2003) indicates that during 1951–2000, landfall hurricane trends are declining for both coasts of the country. Attempts to understand the links between SST changes and inter-annual variations of cyclone formations in western Mexico indicate that the strong El Niño

decades of the 1980s and 1990s appear to have favored fewer storms passing into the central part of the Baja California Peninsula. Diaz et al. (2008), indicate that tropical cyclone contributions to rainfall in the Baja California Peninsula and the State of Sinaloa display a statistically significant correlation with PDO, suggesting a larger contribution of tropical cyclones on annual precipitation in both areas occurs during the positive phase of the PDO than the negative phase.

5. Climate data and quality control

Perhaps, the main difficulty that one encounters when trying to discern regional structures of trends is the lack of sufficient quality records in space and time; this is not an exception in Mexico. According to available information, a little more than 6000 weather stations (Quintas, 2000) and 1475 gauging stations (Banco Nacional de Datos de Aguas Superficiales-BANDAS, 1997) have been put in operation around the country. Unfortunately, only 20% of both kinds of stations have > 40 yrs of records, with datasets on runoff within a river basin (Milly et al., 2005) even smaller than precipitation records (Table 1). The highest density of stations is from 1960 through 2004 (Figure 4) with an abrupt decline at the beginning of the 1980s in both sources of data and slight recovery in rainfall datasets in the 1990s. Considering just those stations with more than four decades of daily observations (between 1920 and 2008), it is still possible to have sufficient information to include all the country (Figure 5) and preserve the longest time series for analysis: 1161 for precipitation and 141 for streamflow data sets. The exception is the Baja California and Yucatan Peninsulas, northwestern Sonora (NWS), and the Altiplano Mexicano, where streamflow observations are scarce or non-existent (Figure 5). Selected basins range from very large (124,000 km²) to very small (25 km²), with an average of 14,500 km². For precipitation records, some parts of the central Baja California Peninsula; NWS; northern Mexico, and mid-level elevations of central Mexico in the Pacific drainage region (near 22° latitude) have no stations with long-term records.

Interval of observations (yr)	Number of stations having data	
	Gauging sites	Weather stations
Less than 1	101 (6.8)	732 (12.1)
1 - 10	442 (30.0)	1139 (18.8)
11 - 20	314 (21.3)	1065 (17.6)
21 - 30	241 (16.3)	1187 (19.6)
31 - 40	165 (11.2)	773 (12.8)
41 - 50	123 (8.3)	664 (11.0)
51 - 60	63 (4.3)	325 (5.4)
61 - 70	25 (1.7)	139 (2.3)
More than 70	1 (0.1)	37 (0.6)
Total	1475 (100)	6061 (100)

Table 1. Density of gauging sites and weather stations with measurements of streamflow and rainfall from 1920–2008. Percentages are shown in parentheses.

	N	C	SE	YP
Annual	402	899	1716	1220
Summer	311 (78)	791 (88)	1446 (84)	955 (79)
Winter	89 (22)	109 (12)	288 (16)	257 (21)

Table 2. The 1921–2008 mean annual and seasonal precipitation (in mm) over each of the domains derived from weather stations displayed in Figure 5. Shown in parentheses is the proportion of seasonal precipitation relative to annual precipitation. N = north domain; C = center domain; SE = southeast domain; YP = Yucatan Peninsula domain.

From daily observations, we calculated total annual (preceding May to following April, the year is of the last month) precipitation and seasonal accumulations for summer (May–October), and winter (November–April) because they are the main precipitation seasons in Mexico (see Figure 3). For each precipitation dataset, we also estimated TDP >0 (expressed in n-days – total days with precipitation >0 mm) for annual and seasonal components. For streamflow records, we estimated mean annual and seasonal streamflow for the same months as precipitation time series. The mean magnitudes of streamflow records, derived from the 141 gauging stations are 295 m^3/s, 374 m^3/s, and 59.1 m^3/s for mean annual, summer, and winter streamflow, respectively. In all variables, a year was considered valid if, at least 85% of the daily records were available (i.e., >310 daily observations for annual series; >156 for summer series, and >153 for winter series), otherwise the year was considered a gap.

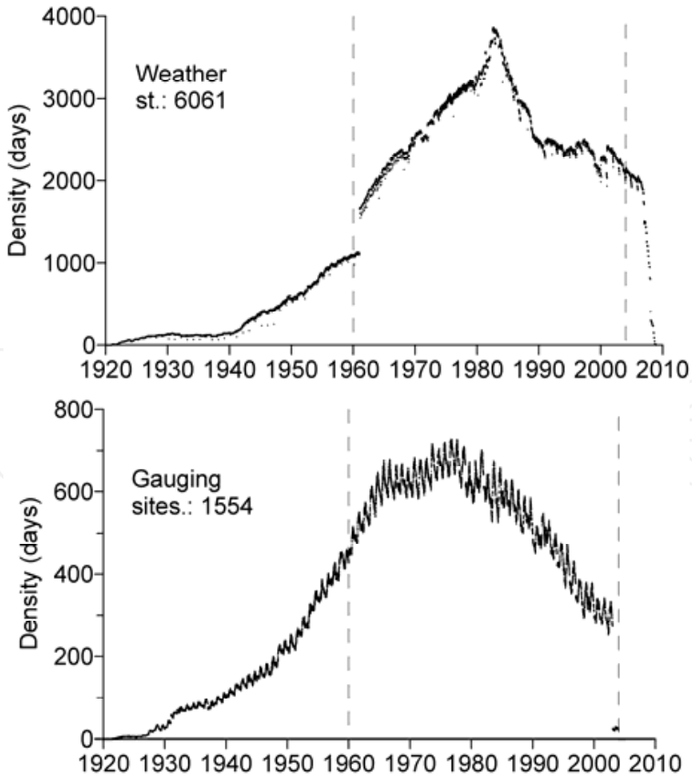

Fig. 4. Series displaying daily density observations of precipitation (a) and streamflow (b) from 1920–2008 derived from 6061 weather and 1554 gauging stations in Mexico.

For all selected datasets, quality control was performed to remove implausible values (i.e., values arising from data entry errors evident as data points with extreme deviations from the overall mean of the series without replication at surrounding station datasets). For streamflow time series, significance tests for variances (*F* distribution) and means (*t*-test distribution) were performed to test for the null hypothesis about the similarity of these parameters inside the series. Hypothesis testing was performed for each series, dividing the series in two equally long parts and comparing the mean and variance of each part. Then, the results were accepted if there were statistically significant differences between the parameters at the 0.05 alpha level. When the series showed significant differences between the parameters, this was considered an indication of change in the long term period.

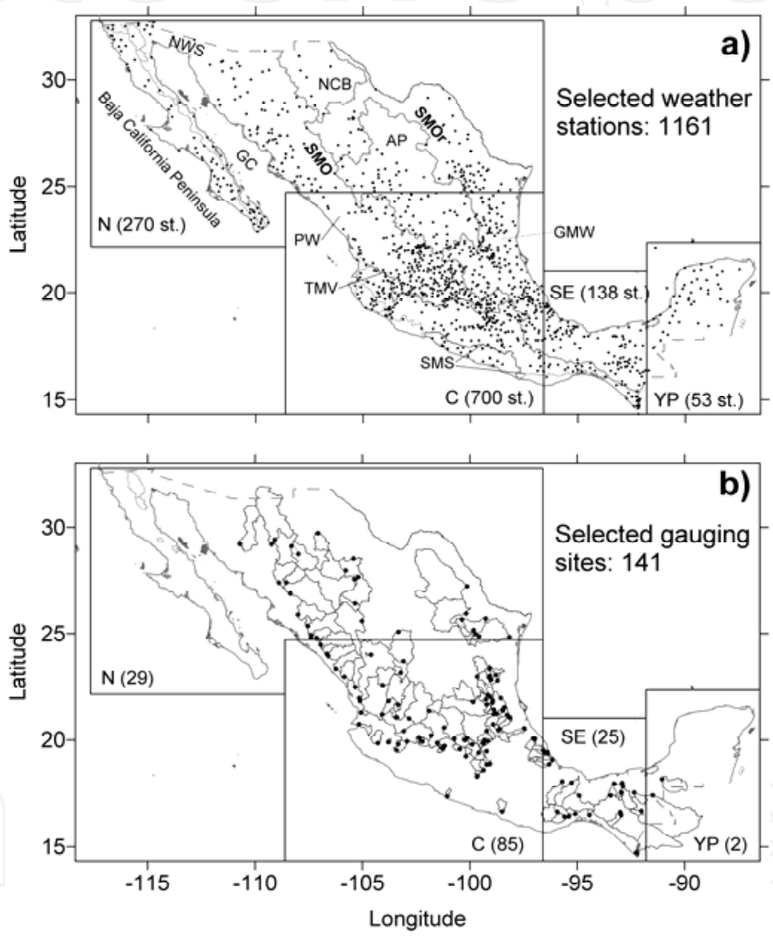

Fig. 5. Spatial distribution of 1161 selected weather stations (a), and 141 selected gauging sites (b) having more than 40 years of records. The maps are divided in domains: N = North; C = Center; SE = Southeast, and YP = Yucatan Peninsula. Density of stations is displayed in parentheses over each domain. Lines in (a) divide the main drainage areas of Mexico: PW = Pacific watershed; GMW = Gulf of Mexico watershed; NCB = northern closed basins; AP = Altiplano Mexicano, and main mountain arrangements: SMO = Sierra Madre Occidental; SMOr = Sierra Madre Oriental; TMVB = Trans-Mexican Volcanic Belt, and SMS = Sierra Madre del Sur. Polygons displayed inside the map in (b) are the catchment areas of each identified gauge point.

Trend analysis was performed for precipitation (total annual and total seasonal observations and their correspondent TDP >0) and streamflow data sets over Mexico from 1161 weather stations and 141 gauging stations (shown in Figure 5), using the procedure explained above. For precipitation time series, our interest was on trends observed in the sequence of days with recorded rainfall (TDP >0). This was done to prove if a station had a declining or increasing trend in total annual and seasonal precipitation corresponding to a downward or upward trend in TDP >0.

6. Regionalization

To simplify the analysis of the regional structure of the trends observed in precipitation and streamflow, the country was divided into polygons of different sizes in the domains (N, C, SE, and YP). Density of weather stations across the domains is displayed in Figure 5. The C domain has the highest density of stations (700 weather stations and 85 gauging sites), while N domain, the largest area, has the lowest density (270 and 29). Climate conditions are different across each of the domains, with a gradient from arid and semi-arid climates over the N domain; sub-humid climates over the C domain, except over the Altiplano Mexicano and middle-to-high elevations in the southeastern part of the C domain, where semi-arid and humid climates dominate, respectively; humid climate over the SE domain, and sub-humid climates over the YP domain (Garcia, 2004). The 1921–2008 mean annual and seasonal precipitation over each domain displays the intra-seasonal differences inside and among the domains (Table 2). As can be seen in Table 2, the arid and semi-arid N domain (annual mean = 402 mm) contrasts with the humid SE domain (1716 mm). The larger winter contribution to annual total is observed over the N domain (22%) followed by the YP domain (21%), the SE domain (16%), and the C domain (12%). This agrees with the larger influence of the intrusion of cold fronts that produce winter precipitation over the N, SE, and YP domains (Figure 3). Each domain is characterized by high annual and seasonal inter-annual variability that is superimposed on multi-decadal variability (Figure 6). Length and magnitude of long-term (multi-decadal) wet and dry periods have been different between the domains, although they overlap in some years. For example (see Figures 6a & b), the prolonged 1940–55 and 1996-onward dry periods in mean total annual precipitation over the C and N domains (early dry period lasting longer in the N domain until 1960, while the actual dry period started earlier in the C domain in 1980); the moderate 1960–1980 wet period between dry periods and the earlier wet period that ended in 1940 over both domains are evidence that wet and dry periods can affect more than half of the country at the same time, affecting not only mean total annual precipitation but also mean total seasonal precipitation (see Figures 6e, f, i & j). These multi-decadal annual and seasonal fluctuations in time series of N and C domains are linked to the PDO shifts, from cold to warm PDO in the mid-1970s and from warm to a temporarily cold PDO at the end of the 1990s (Pavia et al., 2006). Moreover, in the northwestern portion of the N-domain (known as the monsoon region, Higgins et al., 2003), it is known that winter precipitation is in phase with the PDO (Brito-Castillo et al., 2002; Pavia et al., 2006). Stahle et al. (2009) propose that the recent drought (or the 2000s drought) that has affected the N and C domains (Figures 6a, b, e, f, i & j), is associated with a downward trend in precipitation projected for the regions (Seager et al., 2007), based on anthropogenic global warming.

The multi-decadal behavior observed over the SE and YP domains display different structures. Over both domains, dry and wet periods in mean total annual and seasonal precipitation, (see Figures 6c, d, g, h, k & l), appear to last longer, a situation that is unfavorable for Mexico, since over precipitation in both domains is larger (see Table 2) and the effects over the country's national economy might be large, as occurred in the past (Mendoza & Velasco, 2006). Over the SE domain, for example, the early dry period that started in 1926 lasted almost three decades (until the 1950s) and is evident in mean total annual (Figure 6c) and summer (Figure 6g) precipitation. In mean total winter precipitation (Figure 6k), this early dry period ended some years before (mid 1940s). The dry period was followed by a prolonged wet period that occurred from the 1950s onward (Figures 6c, g, k) with a near-normal period at the end of the 1980s-beginning of the 1990s. Comparing the multi-decadal variability between N and SE domains (i.e., Figures 6a, c, e, g, i & k), an apparent opposite pattern emerges (i.e., droughts in the N domain generally coincide with anomalously wet conditions in the SE domain and vice versa) that is related to tropical SST conditions (Matias & Magaña, 2009). The interaction between easterly waves and trade winds over the Gulf of Mexico and the Caribbean Sea appears to be crucial to explain spatial patterns of droughts that affected Mexico (Matias & Magaña, 2009).

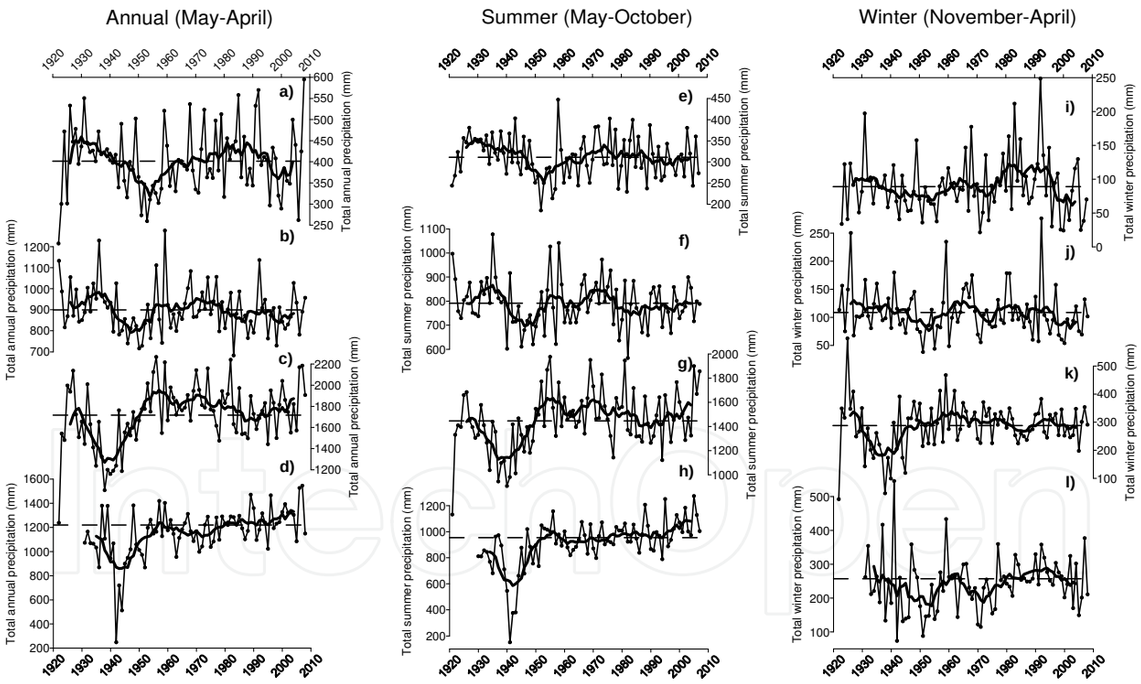

Fig. 6. Mean total annual (May–April) precipitation (left series: a–d; mm), and mean total seasonal precipitation in Mexico for summer (May–October; middle series: e-h) and winter (November–April: right series: i–l), from weather stations displayed in Figure 6 over N-domain (a, e, i); C-domain (b, f, j); SE-domain (c, g, k) and YP-domain (d, h, l). Heavy lines are 9-yr running means and horizontal lines display the mean values over the period for each variable (see Table 2). Note the different ranges in Y-scales due to differences in magnitude and variability in each data set.

7. Regional structures of precipitation trends

The primary goal in detecting trends in streamflow is to identify changes associated with specific physical processes (causal factors) or combinations of processes. But this procedure requires a complete knowledge of the components of the balance equation. Instead, in this study, we start identifying regional trends in precipitation records and then corroborate the corresponding regional trends in streamflow to confirm if they are spatially consistent with one another. This procedure helps, in some way to avoid misleading interpretations, particularly in streamflow datasets where diversion of water for irrigation, control of rivers by damming (when the gauge station is located downstream), or pumping of underground water results in a strong (non-climatic) decline of surface water through time, implying that the causal factor for the declining trend is mostly anthropogenic, and probably with very localized (i.e., non-regional) effects.

Tables 3–5 show the mean magnitude of annual and seasonal trends over each of the domains. In all cases, except in the C domain, total annual precipitation showed a larger number of statistically significant trends than seasonal accumulations. Throughout Mexico, the number of stations displaying downward precipitation trends is larger than stations displaying upward trends, resulting in overall mean annual and summer declining trends. However, the statistical uncertainty in the mean winter trend, based on the 95% confidence interval, includes the zero trend (–0.30 ± 0.54 mm/yr; Table 5). The decrease number of stations having significant trends in winter and their high and uneven spread over the domains (i.e. N, SE and YP) are factors resulted in increasing error in estimating the mean trend, therefore the magnitude of the standard error of trends, derived from weather stations having statistically significant trends in total winter precipitation is very large, indicating that with the available information there is not sufficient evidence to conclude there is an overall mean winter declining trend in Mexico. This conclusion is also valid for the N, SE, and YP domains for mean winter trends (Table 5) and for the SE and YP domains for mean annual (Table 3) and summer (Table 4) trends. In all these cases, the standard error of the trends exceeds the mean magnitude of their respective trends. A different situation occurs over the N and C domains, where the statistical uncertainty of mean annual (Table 3) and summer (Table 4) trends and over the C domain for mean winter trend (Table 5) is smaller than the mean magnitude of the trend. In these cases, we conclude that the mean annual and summer trends are toward increasing precipitation over the N domain and, on the contrary, toward declining precipitation over the C domain (including the mean winter precipitation trend). This last conclusion can be easily verified in Figure 7 that shows the distribution of weather stations over each of the domains that display statistically significant annual (Figure 7a) and seasonal (Figures 7b & c) trends. In all maps of Figure 7, some basic coherent regional trend patterns can be identified for annual and seasonal accumulations over the N domain, such as the tendency for higher precipitation over the high elevations of northeastern Mexico (verified by the line indicating the position of the continental divide, i.e., the limits of the Sierra Madre Oriental), and over middle to high elevations of northwestern Mexico, including the Baja California Peninsula; a tendency for downward precipitation trends over the C domain, with a larger number of stations displaying declining trends over the middle-to-high elevations of the Gulf of Mexico drainage area

than over the Pacific drainage area (except in total winter precipitation, where there is no increasing precipitation trends on either side of the main drainage areas), and over the main drainage area of the Rio Lerma-Santiago basin; a tendency for upward mean seasonal precipitation and downward mean annual precipitation trends over the western half of the YP domain; and finally, a tendency for mean annual and mean summer downward precipitation trends and a mean upward winter precipitation trend over the SE domain. Over the SE domain, individual stations located through the high mountain areas show a tendency for upward trends in annual and seasonal accumulations.

Domain	N(+)	N(-)	Total	Mean Trend (mm/yr)
N	28	7	35	2.54 ± 1.36
C	26	75	101	–3.79 ± 1.57
SE	9	14	23	–3.99 ± 5.40
YP	6	7	13	–0.40 ± 3.76
Overall	69	103	172	–2.38 ± 1.31

Table 3. Mean annual precipitation trends derived from all weather stations having statistically significant trends and located in the North (N), Central (C), Southeast (SE), and Yucatan Peninsula (YP) domains, respectively. N(+) and N(-) are the number of stations displaying upward and downward trends, respectively; the ± values define the 95% confidence intervals for the trends.

Domain	N(+)	N(-)	Total	Mean Trend (mm/yr)
N	22	3	25	2.39 ± 0.26
C	38	69	107	–2.14 ± 1.47
SE	8	12	20	–3.03 ± 4.93
YP	6	3	9	1.90 ± 3.86
Overall	74	87	161	–1.32 ± 1.22

Table 4. Mean summer precipitation trends derived from all the weather stations having statistically significant trends and located in the North (N), Central (C), Southeast (SE), and Yucatan Peninsula (YP) domains respectively. N(+) and N(-) are the number of stations displaying upward and downward trends, respectively; the ± values define the 95% confidence intervals for the trends.

Domain	N(+)	N(-)	Total	Mean Trend (mm/yr)
N	16	6	22	–0.68 ± 0.74
C	10	36	46	–1.13 ± 0.65
SE	9	2	11	0.68 ± 2.03
YP	4	1	5	–0.91 ± 2.14
Overall	39	45	84	–0.30 ± 0.54

Table 5. Mean winter precipitation trends derived from all the weather stations having statistically significant trends located in the North (N), Central (C), Southeast (SE), and Yucatan Peninsula (YP) domains, respectively. N(+) and N(-) are the number of stations displaying upward and downward trends, respectively; the ± values define the 95% confidence intervals for the trends.

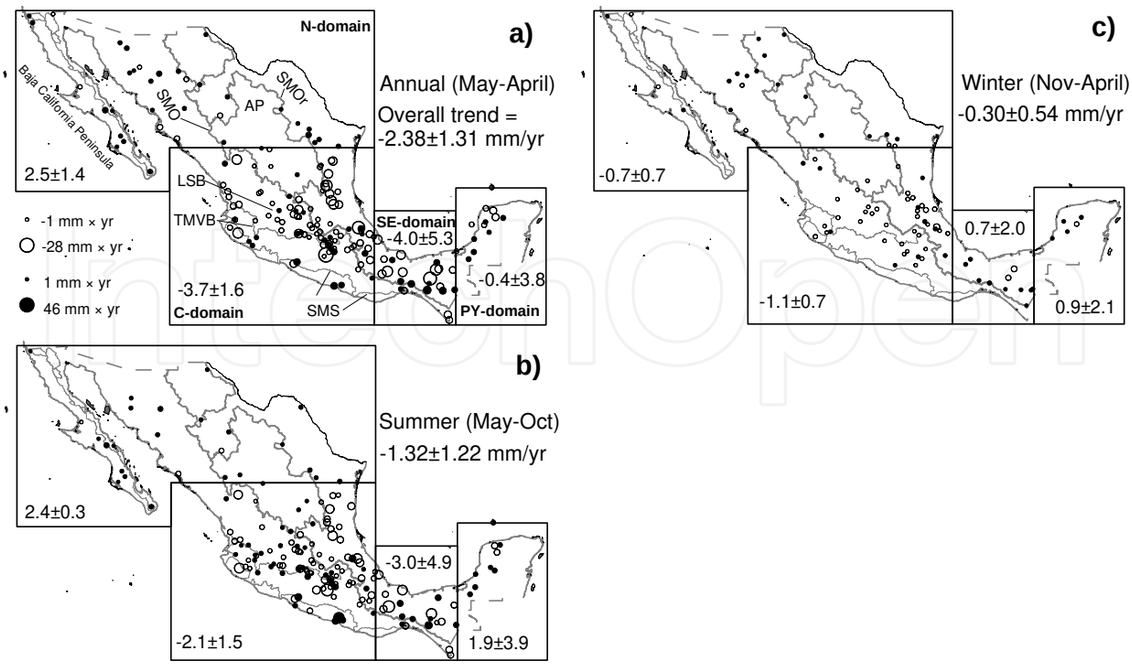

Fig. 7. Maps displaying the distribution of weather stations having statistically significant total annual (a) total summer (b) and total winter (c) precipitation trends in Mexico. Points indicate the position of stations having an increasing precipitation trend while open circles indicate the position of those stations having a declining precipitation trend. Symbols inside the maps are proportional to the magnitude of the trends displayed in the bottom left corner scale of the upper map. The mean trends, derived from the total number of stations overall Mexico, are shown outside the maps, while the mean trends, derived from the stations over each domain, are displayed inside the polygon of each domain (in mm/yr). The ± values define the 95% confidence intervals for the trends. Lines inside the maps show the continental divides with the Pacific drainage areas to the left and Gulf of Mexico drainage areas to the right. Abbreviations in upper left map are the same as in Figure 5a. LSB= Lerma Santiago basin.

To clarify the internal structure of the series, Figures 8–10 show observed time series (expressed as z scores) of selected variables having general significant upward and downward trends. A couple of series have been plotted from each selected station: (1) TDP >0 and (2) total precipitation. Total annual precipitation series are displayed in Figure 8 and total seasonal precipitation time series are displayed in Figures 9 and 10. All series display large inter-annual variability with substantial deviations from linearity in several years. The correspondence between TDP >0 and total annual precipitation trends (having both variables similar general upward or downward trend) is evident in Figure 8 for each station, indicating that an overall upward or downward precipitation trend matches a similar upward or downward trend in TDP >0 (i.e., the decline in total annual precipitation corresponds to a decline in the number of rainy days and vice versa). What is the cause of the overall increasing rainy (dry) days over the N and C domains? It is clear that, if a change of TDP >0 is underway, then a change in annual rainfall accumulation in the same direction

as TDP >0 changes is highly possible and the occurrence of heavy rainfall (from tropical cyclones, for example) only temporarily changes the total annual precipitation without affecting the overall trend.

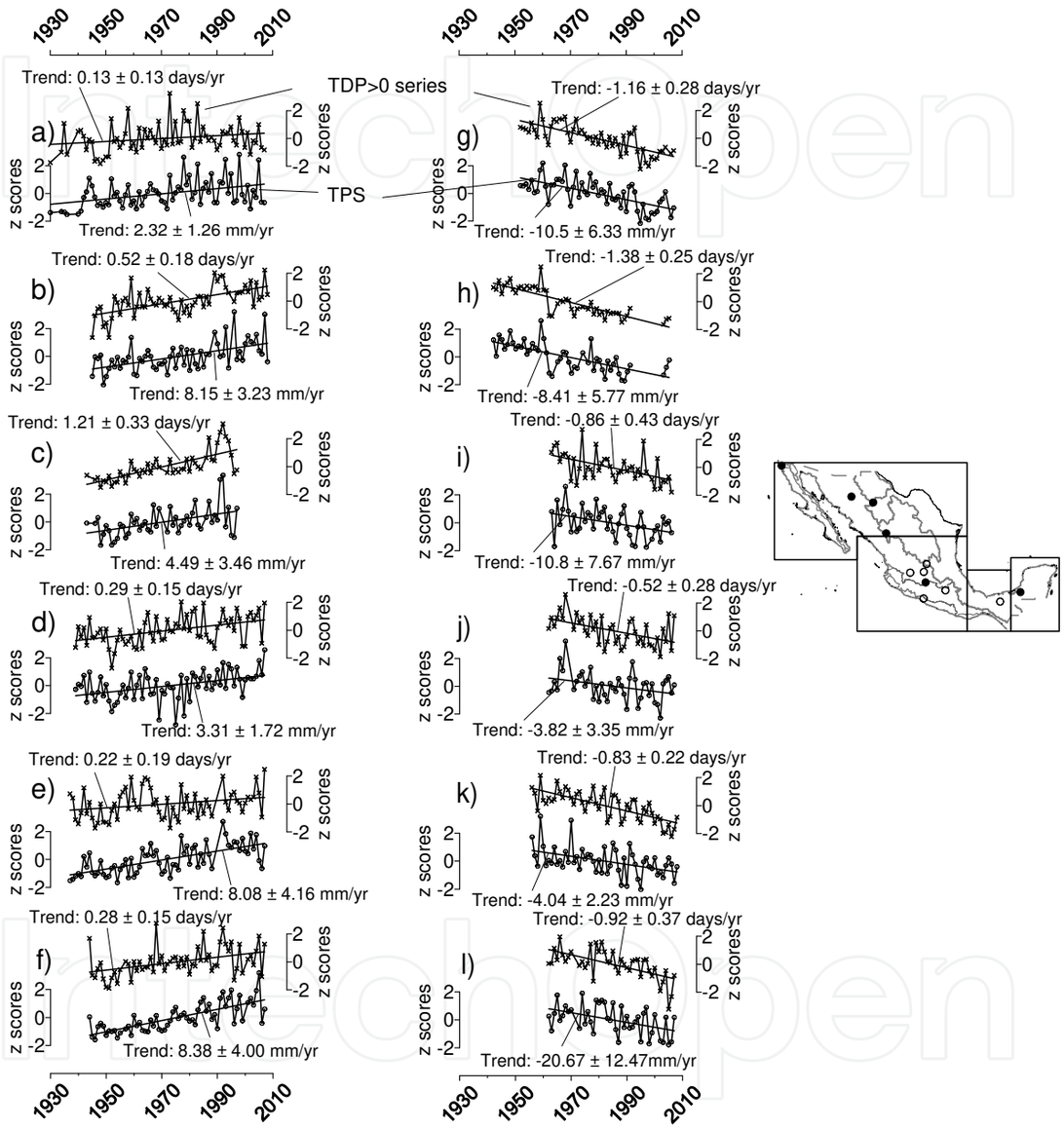

Fig. 8. Examples of observed time series of selected variables (expressed as z scores) displaying upward (left series) and downward (right series) total annual precipitation trends. A couple of series have been plotted from the same selected station, i.e., an upper – TDP >0 (total days with rainfall > 0 mm; lines with ×s) series, and lower TPS-total precipitation series (lines with •). For each variable, the magnitude of the trend with the 95% confidence intervals with their respective units is shown. The map to the right displays the position of the selected stations corresponding to the variables with upward (points) and downward (circles) trends.

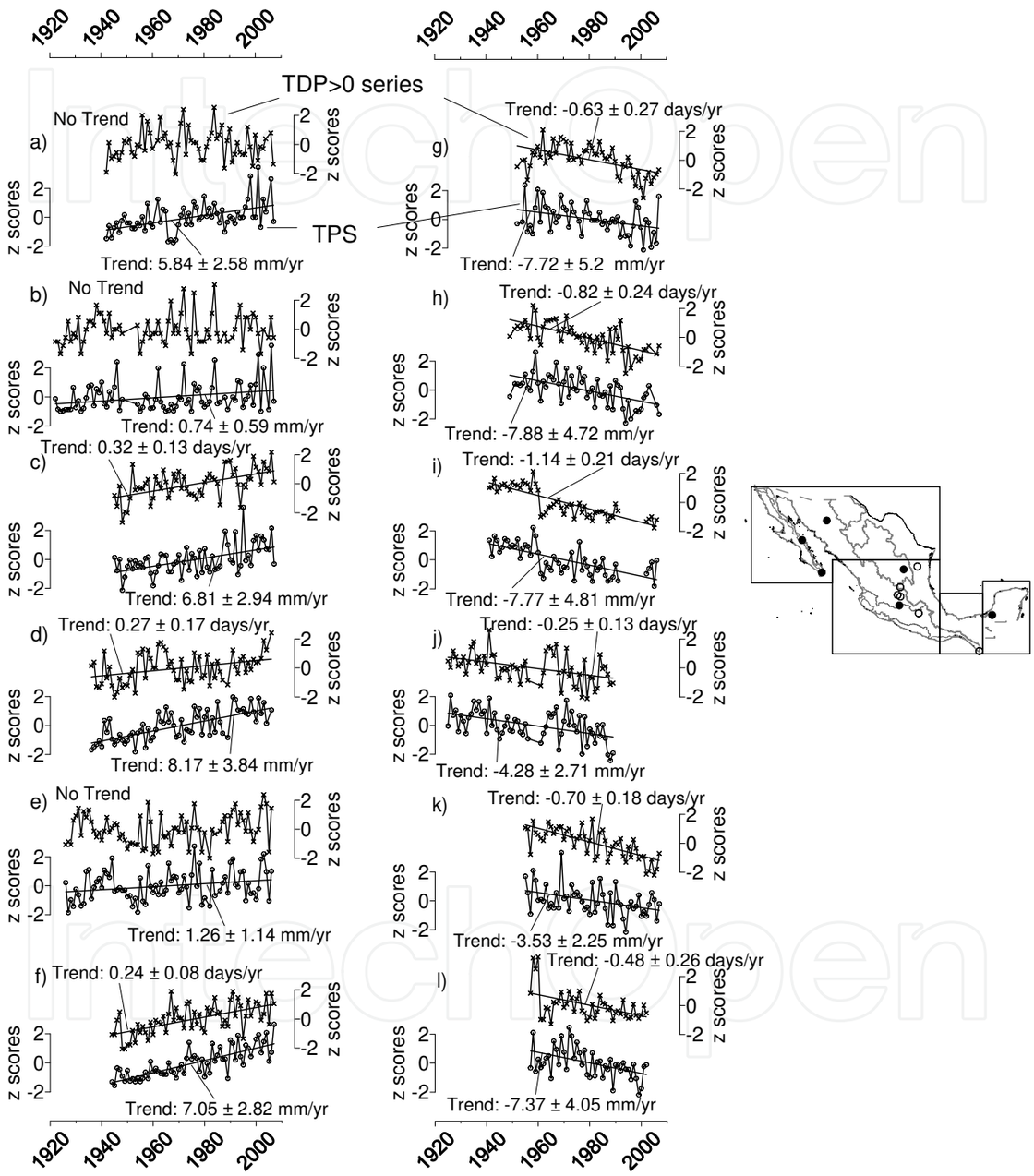

Fig. 9. The same as Figure 8, but for total summer precipitation series. No Trend indicates that for the particular time series the trend is not statistically significant.

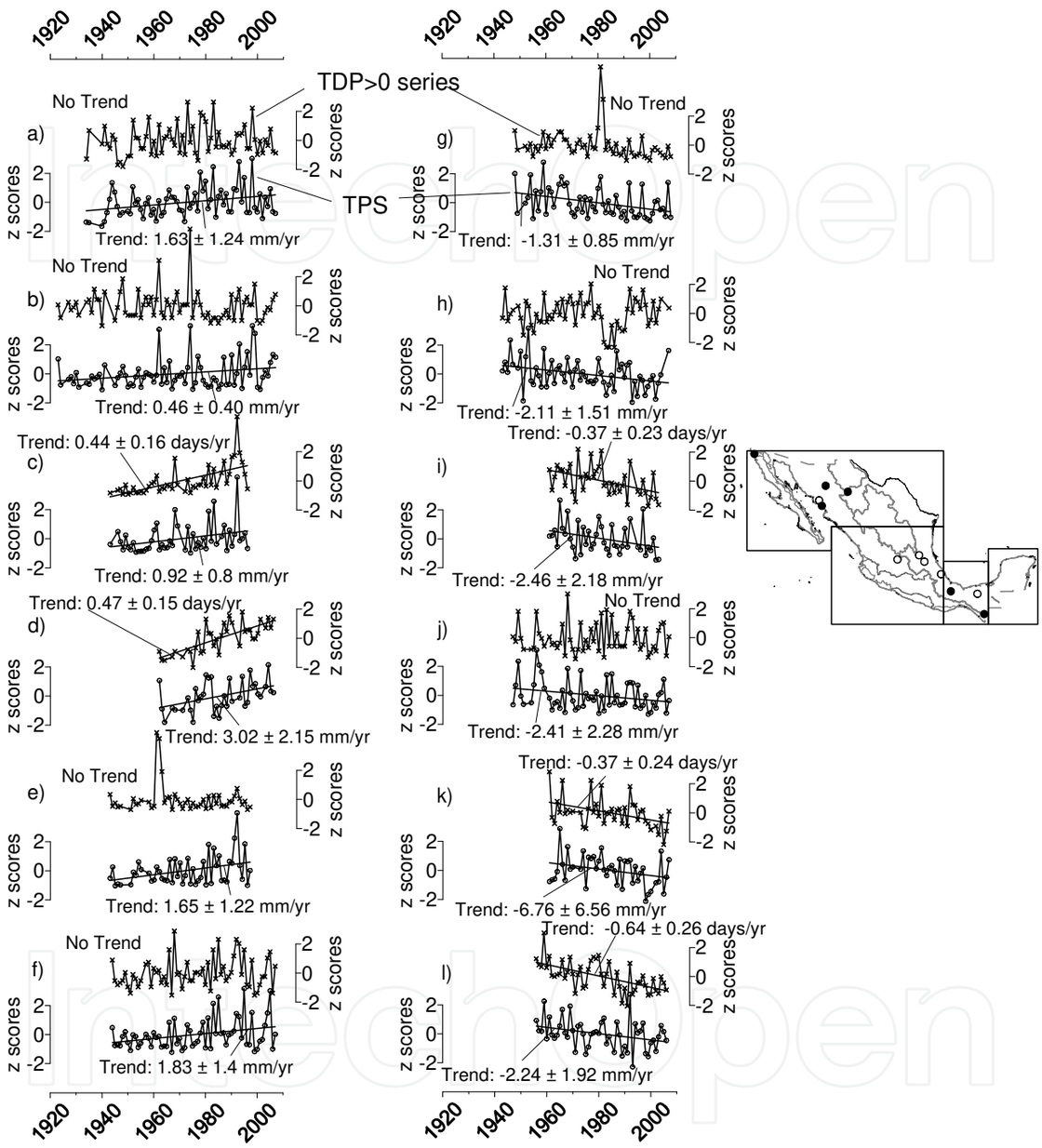

Fig. 10. The same as Figure 8, but for total winter precipitation series. No Trend indicates that for the particular time series the trend is not statistically significant.

This conclusion is not completely valid for total summer (Figure 9) and total winter (Figure 10) precipitation variables because some stations have a general upward or downward seasonal precipitation trend that does not match the corresponding behavior in TDP >0 variables for the same station. This occurs for example, in Figures 9a, 9b, & 9e. Note that the

upper TDP >0 time series in each case does not display statistically significant trends (indicated in Figure 9 by the legend "No Trend"). This is in contrast with the upward trend in the lower total summer precipitation series. In Figures 9a & 9b, a group of years with high precipitation values occurred in recent years, while the corresponding TDP >0 point values show a declining trend in the last two decades, an indication that some external source of humidity has provided the complementary rainfalls for the high summer values recorded in these stations (i.e., less summer rainy days correspond to higher summer rainfalls). This source of precipitation might derive from tropical cyclones, as suggested by Arriaga-Ramírez & Cavazos (2010).

The situation is a little different in winter, where the main source of precipitation proceeds from the passage of cold fronts, enhanced by the southern movement of the subtropical westerly jet stream, which is sometimes associated with El Niño events (Magaña et al., 2003). It is established that there is a direct link between warm SSTs during El Niño years and high winter precipitation in Mexico and vice versa (a cold SSTs during La Niña years and low winter precipitation). In this sense, the high values of winter precipitation during the 1990s, evident in some series (Figures 10a, b, e & f) that display an upward total winter precipitation trend and no trend at all in corresponding the TDP >0 time series might be a reflection of the strong-to-moderate El Niño years of 1991, 1994, 1997, and 2002 that provided necessary atmospheric conditions for production of the complementary winter precipitations in the datasets, since the corresponding TDP >0 time series decreases during the same period. The situation is a little harder to explain in series displaying a decreasing total winter precipitation trend (Figures 10g, h & j), and no trend at all in corresponding TDP >0 time series. The low winter precipitation observed in recent years in these time series might have been influenced by the strong-to-moderate La Niña conditions of 1988, 1998, 1999, and 2007 enhancing the overall decreasing trend, i.e., similar number of rainy days experienced lower precipitation values in recent years.

8. Annual and seasonal regional trends observed in streamflow series

8.1 Hypothesis testing

The results of hypothesis testing (not shown) indicate that changes in variances of all datasets are more common in winter than in summer or annual components. However, a significant change in means or variances of the two halves of the series do not necessarily result in a significant general trend for the series since the number of stations with significant changes in means or variances are always larger than those stations displaying a significant trend. This conclusion is also valid for each domain. On the contrary, similar means or similar variances inside the series do not necessarily mean that the corresponding series does not display a significant overall trend.

8.2 Significant trends in streamflow

Mean winter streamflow show a larger number of stations displaying significant trends than mean summer or mean annual components. Upward trends in streamflow are more common in winter, while downward trends are more common in summer, than the other components.

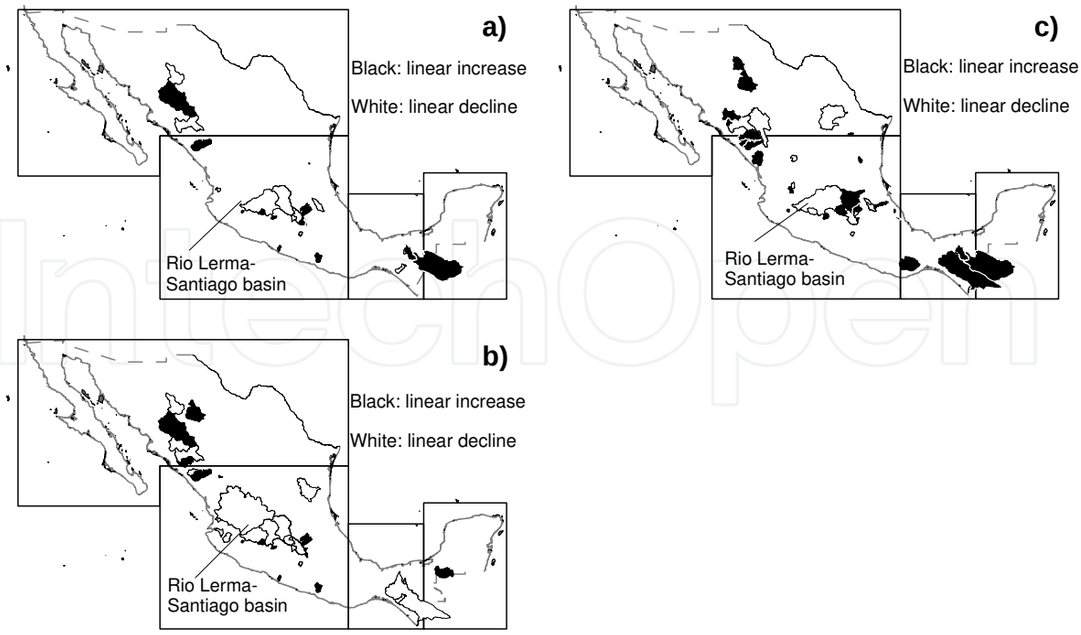

Fig. 11. Maps showing the distribution of river basin polygons displaying significant upward (black polygons) and downward (white polygons) streamflow trends for mean annual (a) mean summer (b) and mean winter (c) components.

The distribution of river basins having significant upward and downward mean annual and mean seasonal streamflow trends is shown in Figure 11. A tendency for a large number of drainage areas to have downward annual and seasonal trends is evident in basins located in the C domain, particularly those in the Lerma-Santiago river basin in central Mexico. This result matches downward trends observed in total annual and seasonal precipitation over the C domain, indicating that overall decreases in rainfall over the C domain have resulted in lower values for streamflow, mainly over Pacific drainage areas. Small basins surrounding the Lerma-Santiago river basin display upward trends in mean annual and seasonal streamflow. Although in the C domain, there are also weather stations displaying significant upward annual and summer trends (See Figures 7a & b), the position of those stations does not necessarily correspond to the position of the small basins. Moreover, mean winter streamflow in some basins display upward trends (Figure 11c), while no weather station displays similar significant upward trends over those areas (Figure 7c). These results suggest that the significant annual and seasonal upward trends in precipitation and streamflow over the C domain might be a reflection of local rather than regional factors. In addition it may be also due to there are 1161 for precipitation and only 141 for streamflow data sets. Not enough streamflow datasets and the large dataset ratio for precipitation to streamflow may cause some errors in the analysis. Over northwestern Mexico in the N domain, large drainage areas display upward and downward mean annual and mean seasonal trends with no obvious regionally coherent pattern (Figures 11a-c). Although we established that the middle-to-high elevations in northwestern Mexico in the N domain have upward mean annual and mean seasonal precipitation trends (Figures 7a-c), the decreasing trends observed in streamflow over these areas do not match this pattern.

Unfortunately, over the drainage areas where significant downward streamflow trends are evident in northwestern Mexico, there are no weather stations (See Figure 5). This makes it impossible to prove a correspondence between precipitation and streamflow variables in western part of the mainland in the N domain.

Finally, some selected time series with significant upward and downward mean annual streamflow trends are displayed in Figure 12. As occurred with total precipitation series, streamflow series also show high inter-annual variability, with substantial deviations from the linear trend. From the time series, it is evident that the dry period during the 1950s (Figures 12a, b, e, i, j & l), and the dry period during the 1990s (Figure 12a, c, h & i) affected a large part of Mexico.

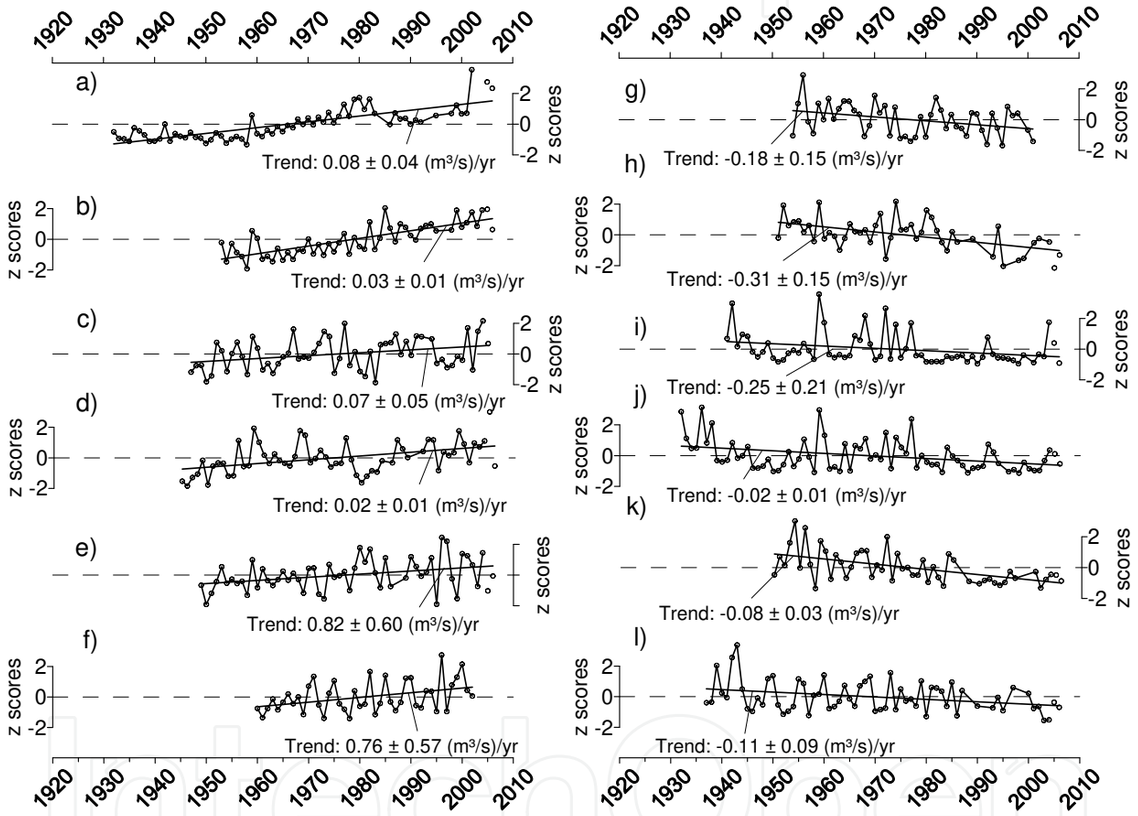

Fig. 12. Examples of observed time series (expressed as z scores) of selected gauging stations displaying upward (left series) and downward (right series) mean annual streamflow trends (lines). The magnitude of each trend with 95% confidence intervals is shown for each variable.

9. Conclusions

Regional changes in rainfall and streamflow in Mexico have significant trends of different sign (Figures 7 & 11), both declining and increasing trends. While isolated differences in trends occur in rainfall and streamflow over large areas, some basic coherent patterns can be identified, such as the trend for lower precipitation in the C domain and a trend for higher precipitation in the N domain. In the C domain, decreasing annual and seasonal trends

match the mean annual and seasonal trends in streamflow. However, we also see that trend structures exhibit some spatial patterns that are not readily explained, such as the trend for declining streamflow in the N domain over large drainage areas of the western mainland and increasing streamflow in the C domain that does not match the opposite behavior of the trends observed in precipitation. The possibility that these differences might be related to more localized external factor and errors resulted from not enough streamflow data sets and the large dataset ratio for precipitation are suggested. However, more detailed analyses are necessary to prove these.

Finally, we conclude that over the last nine decades, Mexico has experienced an overall decrease in mean total annual and summer precipitation, based on analysis of 1161 weather stations across Mexico. Mean total precipitation changes were derived from 172 annual precipitation series and 161 summer rainfall series, displaying significant trends in both directions, declining trends for 103 annual and 87 summer series and increasing trends for 69 annual and 74 summer series. The total change from 1920–2008 has been about 21 mm in mean annual accumulation and 9 mm in mean summer accumulation. The most affected areas from declining precipitation are the middle-to-high elevations in the Gulf of Mexico drainage areas in eastern Mexico and over the upper Rio Lerma-Santiago basin in central Mexico. Several stations in northern and northwestern Mexico (including the Baja California Peninsula), have an overall increase in mean annual and mean summer rainfall accumulations with large variations over the areas. Although the number of stations having declines in mean total winter precipitation is larger than those having increases in mean total winter precipitation, the uncertainties among the trends are so large that the double mean square trend error overpasses the mean magnitude of the trends. In essence, the data does not provide evidence for regional mean changes in winter. The analysis of 141 streamflow series provided more evidence for declines in total annual and summer precipitation, mainly in the Río Lerma-Santiago Basin, although some river basins in northwestern Mexico also display declining trends that do not match the upward trend observed in precipitation. Unfortunately, no weather stations with long datasets are available there, mainly in the highlands of those basins. This makes it difficult to relate streamflow and precipitation changes in northwestern Mexico.

10. Acknowledgments

This work was carried out with the support of the National Council on Science and Technology of Mexico (CONACYT grant J50757-F) and of the Centro de Investigaciones Biologicas del Noroeste (CIBNOR grant PC 0.3). Ira Fogel provided editorial services.

11. References

Arriaga-Ramírez, S. & Cavazos, T. (2010). Regional trends of daily precipitation indices in northwest Mexico and southwest United States. *Journal of Geophysical Research*, Vol. 115, D14111, doi:10.1029/2009JD013248, ISSN 0148-0227

BANDAS (Banco Nacional de Datos de Aguas Superficiales). (1997). Instituto Mexicano de Tecnología del Agua, Período 1997-2004, CD-rom data base, Morelos, México. Available from:<http://www.imta.gob.mx>

Barnett, T.P., Pierce, D.W., AchutaRao, K.M., Gleckler, P.J., Santer, B.D., Gregory, J.M. & Washington, W.M. (2005). Penetration of human-induced warming into the world´s oceans. *Science*, Vol. 309, (July 2005), pp. 284-287, ISSN 0036-8075

Brito-Castillo, L., Díaz, C.S.C. & Ulloa-Herrera, R.S. (2009). Observed tendencies in maximum and minimum temperatures in Zacatecas, Mexico and possible causes. *International Journal of Climatology,* Vol. 29, No. 2, (February 2009), pp. 211-221, ISSN: 1097-0088

Brito-Castillo, L., Douglas, A.V., Leyva-Contreras, A. & Lluch-Belda, D. (2003). The effect of large-scale circulation on precipitation and streamflow in the Gulf of California continental watershed. *International Journal of Climatology*, Vol. 23, No. 7, (June 2003), pp. 751-768, ISSN: 1097-0088

Brito-Castillo, L., Leyva-Contreras, A., Douglas, A.V. & Lluch-Belda, D. (2002). Pacific Decadal Oscillation and the filled capacity of dams on the rivers of the Gulf of California continental watershed. *Atmosfera*, Vol. 15, No. 2, (April 2002), pp. 121-136, ISSN 0187-6236

Díaz, S.C., Salinas-Zavala, C.A. & Hernández-Vázquez, S. (2008). Variability of rainfall from tropical cyclones in northwestern Mexico and its relation to SOI and PDO. *Atmosfera*, Vol. 21, No. 2, (April 2008), pp. 213-223, ISSN 0187-6236

Douglas, A.V. & Englehart, Ph. J. (2007). A Climatological perspective of transient synoptic features during NAME 2004. *Journal of Climate*, Vol. 20, No. 9, (May 2007), pp. 1947-1954, ISSN 0894-8755

Englehart, Ph.J. & Douglas, A.V. (2004). Characterizing regional-scale variations in monthly and seasonal surface air temperature over Mexico. *International Journal of Climatology,* Vol. 24, No. 15, (December 2004), pp. 1897-1090, ISSN: 1097-0088

Farfan, L.M. & Zehnder J.A. (1994). Moving and stationary mesoscale convective systems over Northwest Mexico during the southwest area monsoon project. *Weather and Forecasting*, Vol. 9, No. 4, (December 1994), pp. 630-639, ISSN: 0882-8156

Farfan, L.M. (2011). Eastern Pacific tropical cyclones and their impact over western Mexico. In: *Experimental and Theoretical Advances in Fluid Dynamics*, Klapp et al. (eds.), Environmental Science and Engineering, pp. 135-148, doi: 10.1007/978-3-642-17958-7_9. ISBN: 978-3-642-17957-0, Springer-Verlag Berlin Heidelberg

Garcia, E. (2004). *Modificaciones al sistema de clasificación climática de Koppen (para adaptarlo a las condiciones climáticas de México)*. 5ta edición, Instituto de Geografía, UNAM, ISBN: 970-32-1010-4, México, D.F.

Giovannettone, J.P. & Barros, A.P. (2008). A remote sensing survey of the role of landform on the organization of orographic precipitation in Central and southern Mexico. *Journal of Hydrometeorology*, Vol. 9, No. 6, (December 2008), pp. 1257-1283, ISSN: 1525-7541

Gutierrez-Ruacho, O.G., Brito-Castillo, L., Díaz, C.S.C. & Watts Ch. (2010). Trends in rainfall and extreme temperatures in Northwestern Mexico. *Climate Research,* Vol. 42, No. 2, (July 2010),pp. 133-142, ISSN: 1616-1572

Higgins, R.W., Douglas, A.V., Hahmann, A., Berbery, E.H., Gutzler, D., Shuttleworth, J., Stensrud, D., Amador J., Carbone, R., Cortez, M., Douglas, M., Lobato, R., Meitin, J., Ropelewski, Ch., Schemm, J., Schubbert, S. & Zhang, Ch. (2003). Progress in Pan American CLIVAR research: the North American monsoon system. *Atmosfera*, Vol. 16, No. 1, (January 2003), pp. 29-65, ISSN 0187-6236

Houghton, J.T., Ding, Y., Griggs, D.J., Noguer, M., van der Linden, P.J., Dai, X., Maskell, K. & Johnson, C.A. (2001). *Climate Change 2001: The Scientific Basis*, Cambridge University Press, ISBN: 9780521014953, Cambridge, U.K.

IPCC (2007). Intergovernmental Panel on Climate Change. In *Climate Change 2007: The physical science basis. Contribution of working group I to the fourth assessment report of the IPCC (AR4)*, Solomon, S., Qin, D., Manning, M., Chen, Z., Marquis, M., Avery, K.B., Tignor, M. & Miller, H.L. (eds). Cambridge University Press, New York, http://www.ipcc.ch/press/index.htm

Jáuregui, E. (2003). Climatology of landfalling hurricanes and tropical storms in Mexico. *Atmosfera*, Vol. 16, No. 4, (October 2003), pp. 193-204, ISSN 0187-6236

Knutson, Th.R., McBride, J.L Greenhouse Gases / Book 1., Chan, J., Emanuel, K., Hollan, G., Landsea, Ch., Held, I., Kossin, J.P., Srivastava A.K. & Sugi, M. (2010). Tropical cyclones and climate change. *Nature*, Vol. 3, (March 2010), pp. 157-163, ISSN: 0028-0836

Lindzen, R.S. (2007). Taking greenhouse warming seriously. *Energy & Environment*, Vol. 18, No. 7+8, pp. 937-950, ISSN: 0958-305X

Magaña, V., Amador, J. & Medina, S (1999). The midsummer drought over Mexico and Central America. *Journal of Climate*, Vol. 12, No. 6, (June 1999), pp. 1577-1588, ISSN 0894-8755

Magaña, V.O., Vázquez, J.L, Pérez, J.L. & Pérez, J.B. (2003). Impact of El Niño on precipitation in Mexico. *Geofísica Internacional*, Vol. 42, No. 3, pp. 313-330, ISSN: 0016-7169

Matías, M. & Magaña, V. (2010). Regional aspects of prolonged meteorological droughts over Mexico and Central America. *Journal of Climate*, Vol. 23, No. 5 (March 2010), pp. 1175-1188, ISSN 0894-8755

McBride, J.L. (1995). *Tropical cyclone formation, global perspective on tropical cyclones*. Elsberry, R.L. (ed.). World Meteorological Organization, pp. 106-197

Mendoza, B. & Velasco, V. (2006). A study of historical droughts in southeastern Mexico. *Journal of Climate*, Vol. 19, No. 12 (June 2006), pp. 2916-2934, ISSN 0894-8755

Milly, P.C.D., Dunne, K.A & Vecchia, A.V. (2005). Global pattern of trends in streamflow and water availability in a changing climate. *Nature*, Vol. 438, (November 2005), pp. 347-350, ISSN: 0028-0836

Pavia, E.G., Graef F. & Reyes, J. (2009). Annual and seasonal surface air temperature trends in Mexico. *International Journal of Climatology,* Vol. 29, No. 9, (July 2009), pp. 1324-1329, ISSN: 1097-0088

Pavia, E.G., Graef, F. & Reyes, J. (2006). PDO-ENSO effects in the climate of Mexico. *Journal of Climate*, Vol. 19, pp. 6433-6438, doi:10.1175/JCL14045.1, ISSN 0894-8755

Quintas, I. (2000). ERIC II. In: *Documentación de la base de datos climatológica y del programa extractor (ERIC II: Documentation of the climatologic database anda data extraction program)*. Instituto Mexicano de Tecnología del Agua (IMTA). 54 pp.

Seager, R., Tign, M., Held, I., Kushnir, Y., Lu, J., Vecchi, G., Huan, H., Harnik, N., Leetmaa, A., Lau, N., Li, C. Velez, J. & Naik, N. (2007). Model projections of an imminent transition to a more arid climate in southwestern North America. *Science*, Vol. 316, (May 2007), pp. 1181-7784, ISSN 0036-8075

Stahle, D.W., Cook, E.R., Villanueva-Diaz, J., Fye, F.K, Burnette, D.J., Griffin, R.D., Acuña-Soto, R., Seager, R. & Heim, Jr., R.R. (2009). Early 21st-century drought in Mexico, *Eos Translational*, AGU, Vol. 90, No. 11, pp. 89-100, doi:10.1029/2009EO110001

Trenberth, K. (2005). Uncertainty in Hurricane and global warming. *Science*, Vol. 308, (June 2005), pp. 1753-1754, ISSN 0036-8075

Turrent, C. & Cavazos, T. (2009). Role of the land-sea thermal contrast in the interannual modulation of the North American Monsoon. *Geophysical Research Letters*, Vol. 36, L02808, doi:10.1029/2008GL036299, ISSN: 0094-8276

Wang, C., Lee, S.K & Enfield, D.B. (2007). Impact of the Atlantic warm pool on the summer climate of the western hemisphere. *Journal of Climate*, Vol. 20, No. 20, (October 2007), pp. 5021-5040, ISSN 0894-8755

Webster, P.J., Hollan, G.J., Curry, J.A. & Chang, H.-R. (2005). Changes in tropical cyclone number, duration and intensity in a warming environment. *Science*, Vol. 309, (September 2005), pp. 1844-1846, ISSN: 0036-8075

Weiss, J.L. & Overpeck, J.T. (2005). Is the Sonoran Desert losing its cool?. *Global Change Biology,* Vol. 11, No. 12, (December 2005), pp. 2065-2077., ISSN: 1365-2486

Wigley, T.M.L. (2006). Appendix A: Statistical Issues Regarding Trends. *In Temperature Trends in the Lower Atmosphere: Steps for Understanding and Reconciling Differences.* TR Karl, SJ Hassol, CD Miller, and WL Murray (Eds.). A Report by the Climate Change Science Program and the Subcommitttee on Global Change Research,Washington, DC. 165 pp.

Yu, J., Wang, Y. & Hamilton, K. (2010). Response of tropical cyclone potential intensity to al global warming scenario in the IPCC AR4 CGCMs. *Journal of Climate*, Vol. 23, No. 6, (March 2010), pp. 1354-1373, ISSN: 0894-8755

Zhao, X. (2011). Is global warming mainly due to anthropogenic greenhouse gas emissions?. *Energy Sources, Part A: Recovery, Utilization, and Environmental Effects*, Vol. 33, No. 21, (August 2011), pp. 1985-1992, ISSN: 1556-7036

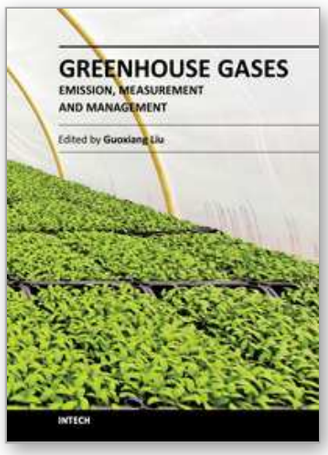

Greenhouse Gases - Emission, Measurement and Management
Edited by Dr Guoxiang Liu

ISBN 978-953-51-0323-3
Hard cover, 504 pages
Publisher InTech
Published online 14, March, 2012
Published in print edition March, 2012

Understanding greenhouse gas sources, emissions, measurements, and management is essential for capture, utilization, reduction, and storage of greenhouse gas, which plays a crucial role in issues such as global warming and climate change. Taking advantage of the authors' experience in greenhouse gases, this book discusses an overview of recently developed techniques, methods, and strategies: - A comprehensive source investigation of greenhouse gases that are emitted from hydrocarbon reservoirs, vehicle transportation, agricultural landscapes, farms, non-cattle confined buildings, and so on. - Recently developed detection and measurement techniques and methods such as photoacoustic spectroscopy, landfill-based carbon dioxide and methane measurement, and miniaturized mass spectrometer.

InTech Europe
University Campus STeP Ri
Slavka Krautzeka 83/A
51000 Rijeka, Croatia
Phone: +385 (51) 770 447
Fax: +385 (51) 686 166
www.intechopen.com

InTech China
Unit 405, Office Block, Hotel Equatorial Shanghai
No.65, Yan An Road (West), Shanghai, 200040, China
中国上海市延安西路65号上海国际贵都大饭店办公楼405单元
Phone: +86-21-62489820
Fax: +86-21-62489821

IntechOpen